Agronomy & Horticulture -- Faculty Publications   Agronomy and Horticulture Department

2006

Mutations in Arabidopsis *Yellow Stripe-Like1* and *Yellow Stripe-Like3* Reveal Their Roles in Metal Ion Homeostasis and Loading of Metal Ions in Seeds

Brian M. Waters
University of Nebraska-Lincoln, bwaters2@unl.edu

Heng-Hsuan Chu
University of Massachusetts

Raymond J. DiDonato
University of Massachusetts

Louis A. Roberts
University of Massachusetts

Robynn B. Eisley
University of Massachusetts

Follow this and additional works at: https://digitalcommons.unl.edu/agronomyfacpub

See next page for additional authors

Part of the Agricultural Science Commons, Agriculture Commons, Agronomy and Crop Sciences Commons, Botany Commons, Horticulture Commons, Other Plant Sciences Commons, and the Plant Biology Commons

Waters, Brian M.; Chu, Heng-Hsuan; DiDonato, Raymond J.; Roberts, Louis A.; Eisley, Robynn B.; Lahner, Brett; Salt, David E.; and Walker, Elsbeth L., "Mutations in Arabidopsis *Yellow Stripe-Like1* and *Yellow Stripe-Like3* Reveal Their Roles in Metal Ion Homeostasis and Loading of Metal Ions in Seeds" (2006). *Agronomy & Horticulture -- Faculty Publications*. 1046.
https://digitalcommons.unl.edu/agronomyfacpub/1046

Authors

Brian M. Waters, Heng-Hsuan Chu, Raymond J. DiDonato, Louis A. Roberts, Robynn B. Eisley, Brett Lahner, David E. Salt, and Elsbeth L. Walker

Mutations in Arabidopsis *Yellow Stripe-Like1* and *Yellow Stripe-Like3* Reveal Their Roles in Metal Ion Homeostasis and Loading of Metal Ions in Seeds

Brian M. Waters,[1,3] Heng-Hsuan Chu,[1] Raymond J. DiDonato,[1,4]
Louis A. Roberts,[1,5] Robynn B. Eisley,[1] Brett Lahner,[2]
David E. Salt,[2] and Elsbeth L. Walker[1]

1. Biology Department, University of Massachusetts, Amherst, Massachusetts 01003
2. Center for Plant Environmental Stress Physiology, Purdue University, West Lafayette, Indiana 47907
3. *Present address:* Department of Pediatrics-Nutrition, Baylor College of Medicine, Houston, TX 77030
4. *Present address:* Microbiology Department, University of Massachusetts, Amherst, MA 01003
5. *Present address:* Biochemistry and Molecular Biology Department, University of Massachusetts, Amherst, MA 01003

Corresponding author – Elsbeth L. Walker, email ewalker@bio.umass.edu

Abstract

Here, we describe two members of the Arabidopsis (*Arabidopsis thaliana*) Yellow Stripe-Like (YSL) family, *AtYSL1* and *AtYSL3*. The YSL1 and YSL3 proteins are members of the oligopeptide transporter family and are predicted to be integral membrane proteins. YSL1 and YSL3 are similar to the maize (*Zea mays*) YS1 phytosiderophore transporter (ZmYS1) and the AtYSL2 iron (Fe)-nicotianamine transporter, and are predicted to transport metal-nicotianamine complexes into cells. *YSL1* and *YSL3* mRNAs are expressed in both root and shoot tissues, and both are regulated in response to the Fe status of the plant. β-Glucuronidase reporter expression, driven by *YSL1* and *YSL3* promoters, reveals expression patterns of the genes in roots, leaves, and flowers. Expression was highest in senescing rosette leaves and cauline leaves. Whereas the single mutants *ysl1* and *ysl3* had no visible phenotypes, the *ysl1ysl3* double mutant exhibited Fe deficiency symptoms, such as interveinal chlorosis. Leaf Fe concentrations are decreased in the double mutant, whereas manganese, zinc, and especially copper concentrations are elevated. In seeds of double-mutant plants, the concentrations of Fe, zinc, and copper are low. Mobilization of metals from leaves during senescence is impaired in the double mutant. In addition, the double mutant has reduced fertility due to defective anther and embryo development. The proposed physiological roles for YSL1 and YSL3 are in delivery of metal micronutrients to and from vascular tissues.

Metal micronutrients fulfill critical biochemical and structural roles in plants. Iron (Fe) is a required nutrient for nearly all organisms. Fe can be readily reduced or oxidized in biochemical reactions, making it well suited for its role in redox-active proteins involved in respiration, photosynthesis, and nitrogen (N) fixation (Hell and Stephan, 2003). Fe is also vital for completion of the citric acid cycle, assimilation of sulfur (S) and N, and chlorophyll biosynthesis. Copper (Cu) is a component of several important proteins, such as tyrosinase, cytochrome C oxidase, Cu,Zn-superoxide dismutase, and the ethylene receptor ETR1. Zinc (Zn) is an important structural component of protein domains such as Zn fingers found in many DNA-binding proteins, as well as enzymes such as alcohol dehydrogenase. Manganese (Mn) is a key component of the photosynthetic apparatus.

In recent years, much has been learned about the genes and proteins necessary for primary Fe and Zn uptake from the soil (Curie and Briat, 2003; Schmidt, 2003). Strategy II plants (the grasses) obtain Fe by secretion of Fe(III)-binding molecules, called phytosiderophores, and then by taking the Fe(III)-phytosiderophore complex into the root cells. Genes for phytosiderophore synthesis have been identified (Higuchi et al., 1999, 2001; Kobayashi et al., 2001; Inoue et al., 2003), and a gene for Fe(III)-phytosiderophore uptake, *ZmYS1*, has been identified in maize (*Zea mays*; Curie et al., 2001). Strategy I plants (nongrasses, including Arabidopsis [*Arabidopsis thaliana*]) obtain Fe by lowering the rhizosphere pH using H^+-ATPase proteins, by reducing Fe(III) to Fe(II) with ferric reductase proteins, and by taking up the reduced Fe using Fe(II) transporter proteins (Curie and Briat, 2003; Hell and Stephan, 2003). Ferric reductase genes have been identified in *Arabidopsis* and several other plant species (Robinson et al., 1999; Waters et al., 2002; Li et al., 2004), as have Fe(II) transporter genes of the ZIP family (Eide et al., 1996; Eckhardt et al., 2001; Vert et al., 2001; Bughio et al., 2002; Cohen et al., 2004). ZIP family genes are likely to be the primary proteins responsible for Zn uptake from the rhizosphere (Grotz et al., 1998). Primary uptake of Cu and Mn has been less thoroughly studied, although several ZIP family proteins have been demonstrated to be capable of transporting Mn (Guerinot, 2000).

Despite this progress, little is known about how metals are translocated and assimilated following import into the root. Mutants with defects in homeostatic regulation of Fe and other metals have been studied for several years. The *Arabidopsis* mutant *man1* (Delhaize, 1996), also called *frd3* (Rogers and Guerinot, 2002), was discovered on the basis of Mn overaccumulation in the leaves, which resulted in a chlorotic phenotype. More recently, it has been shown that the FRD3 protein controls Fe localization within the plant (Green and Rogers, 2004). The pea (*Pisum sativum*) mutant *bronze* (*brz*) overaccumulates Fe, Cu, Mn, Zn, and other elements in shoots (Welch and LaRue, 1990; Cary et al., 1994), and the pea mutant *degenerative leaves* (*dgl*) overaccumulates Fe in leaves and seeds and has altered shoot-to-root signaling

of Fe status (Grusak and Pezeshgi, 1996). Both pea mutants exhibit constitutive root ferric reductase activity (Grusak et al., 1990; Grusak and Pezeshgi, 1996) and transcript expression (Waters et al., 2002). The genes for *brz* and *dgl* remain unidentified. The tomato (*Lycopersicon esculentum*) mutant *chloronerva* (*chln*) exhibits interveinal chlorosis and defects in metal accumulation and translocation (Stephan and Scholz, 1993). The underlying cause of this phenotype is the absence of nicotianamine (NA) due to a mutation in the NA synthase gene (Ling et al., 1999).

NA is a nonprotein amino acid that is ubiquitous in both strategy I and strategy II plants. Based on studies of the *chln* mutant, NA is vital for homeostasis of Fe and other metal micronutrients. The *chln* mutant exhibits increased ferric reductase activity and overaccumulates Fe in mature leaves (Stephan and Grun, 1989), yet its younger leaves are chlorotic (Becker et al., 1992). A recent study in tobacco (*Nicotiana tabacum*) used the NA aminotransferase (*NAAT*) gene of barley (*Hordeum vulgare*), which converts NA to a precursor of mugeneic acids. Overexpression of *NAAT* in tobacco resulted in a phenotype similar to *chln* because all detectable NA was consumed by NAAT (Takahashi et al., 2003). This transgenic *naat* tobacco exhibited interveinal chlorosis; lower levels of Fe, Cu, Mn, and Zn in young leaves; and had abnormal flower development resulting in sterility.

In previous work, our group has demonstrated that *ZmYS1* and *AtYSL2* are capable of transporting Fe(II)- NA into cells (Curie et al., 2001; DiDonato et al., 2004; Roberts et al., 2004), and others have shown that *OsYSL2* of rice (*Oryza sativa*) can transport Fe(II)-NA (Koike et al., 2004). Here, we use a genetic approach to show that the combination of null mutations in two *AtYSL*s, *YSL1* and *YSL3*, results in a severe phenotype that includes interveinal chlorosis; altered metal concentrations in leaves, roots, and seeds; and greatly decreased fertility. *YSL* promoter-*β-glucuronidase* (*GUS*) reporter constructs reveal a localization pattern that is consistent with a role for YSL1 and YSL3 in providing metal-NA compounds to leaves, pollen, and developing seeds.

Results

Single Mutants Have No Apparent Phenotype, and Double Mutants Exhibit Interveinal Chlorosis

Within the Arabidopsis YSL family, the YSL1 and YSL3 proteins are most closely related to YSL2 (DiDonato et al., 2004). However, the gene structure of these three family members is dissimilar: *YSL1* has only four exons, whereas *YSL2* has six exons and *YSL3* has seven exons (fig. 1A). Thus, the gene structure suggests that these genes are evolutionarily distant, but conservation of the protein sequences suggests that the proteins perform similar functions.

Salk T-DNA insertion mutants *ysl1-2* (SALK_034534) and *ysl3-1* (SALK_064683) were confirmed to have T-DNA insertions by PCR and sequencing, and homozygous lines were isolated and confirmed to be null mutations by absence of mRNA, as determined by reverse transcription (RT)-PCR (Le Jean et al., 2005; data not shown). Insertion of the T-DNA occurs in exon 4 in *ysl1-2* (Le Jean et al., 2005) and in exon 7 in *ysl3-1* (fig. 1A). Crosses between homozygous *ysl1-2* and *ysl3-1* were performed, and homozygous *ysl1ysl3* double mutants were identified among F2 individuals by PCR. Wild-type plants were Columbia (Col-0).

Growth of Salk T-DNA insertion mutants *ysl1-2* and *ysl3-1* on Murashige and Skoog (MS) agar and soil did not reveal noticeable differences between the mutants and wild-type Col-0 plants (data not shown). However, when double mutants were constructed by crossing, a phenotype was readily observable. After approximately 2 weeks on MS agar plates or soil, the *ysl1ysl3* mutants were noted to have chlorotic leaves, with an interveinal chlorosis pattern resembling that of Fe deficiency (fig. 1, B and C), although on plates the green vein pattern was more pronounced than that of –Fe-grown wild-type plants (fig. 1, D–F). Unlike typical Fe deficiency, the chlorosis was not especially pronounced in the youngest leaves and was most apparent during leaf expansion. Supplementation of Sequestrene (Fe-EDDHA) to soil-grown plants corrected the chlorotic phenotype, suggesting that Fe deficiency was the cause of chlorosis. Transgenic plants carrying a wild-type YSL3 gene with a carboxyl-terminal green fluorescent protein tag had normal leaf pigmentation (five independent lines examined in the T2 generation; data not shown), demonstrating that the mutant phenotype is complemented by YSL3.

YSL1 *and* YSL3 *Are Metal Regulated*

Most genes that are involved in Fe uptake are regulated by the Fe status of the plant such that the transcript levels increase when the plant is Fe deficient (Eide et al., 1996; Robinson et al., 1999; Eckhardt et al., 2001; Vert et al., 2001; Bughio et al., 2002; Waters et al., 2002; Cohen et al., 2004; Li et al., 2004). We wondered whether *YSL1* and *YSL3* are also regulated by Fe or other metals. To test this, we grew plants for 7 d on full MS agar, then transferred them to MS (control), MS lacking Cu, Zn, or Mn for 7 d, or MS lacking Fe for 3, 5, or 7 d. At these times, roots and shoots were harvested and weighed, and RNA was extracted and used for RT-PCR (fig. 2). *YSL1* and *YSL3* transcripts had similar regulation patterns. In shoots, both *YSL1* and *YSL3* message levels appeared to be slightly increased by deficiencies of Cu, Mn, or Zn, whereas message levels markedly declined after 3, 5, and 7 d of growth on –Fe plates (fig. 2A). In roots, little difference in *YSL1* or *YSL3*

transcript levels was observed as a result of any of the treatments, although, as expected, the steady-state level of *IRT1* mRNA was increased by the –Fe treatments (fig. 2B). *YSL3* was more abundant in roots than *YSL1*, based on the intensity of the PCR product. In roots, twice as much template and 35 cycles were required to detect *YSL1*, whereas only 30 cycles were required for *YSL3*. The metal regulation pattern of *YSL1* and *YSL3* was similar to that of *YSL2* (DiDonato et al., 2004), suggesting similar physiological roles for these three genes.

Expression Patterns of YSL1 *and* YSL3

To determine tissue expression patterns of *YSL1* and *YSL3*, gene promoters were fused to *GUS* and transformed into Col-0 plants. Plants were grown on MS plates or soil and various tissues at different stages of the plant life cycle were observed for GUS activity (fig. 3, A–L). In leaves, both *YSL1* and *YSL3* had similar expression patterns, with GUS staining observed primarily in the veins and the cells surrounding veins. The vascular parenchyma cells surrounding the entire vein were stained (fig. 3L). No staining was observed directly in either xylem or phloem cells. We also noted that the youngest leaves did not stain for GUS with the intensity of older leaves. In roots, staining was less intense, but was observed in the vascular cylinder for both *YSL1* and *YSL3*. Differences in expression patterns between these two genes were most obvious in floral tissues. For *YSL1*, GUS staining was observed in the pedicel, sepals, and faintly in petals (fig. 3C). Staining was also observed in immature anthers (but not mature anthers; fig. 3D) and in filaments of mature stamens (fig. 3C). The vasculature of the pistil also exhibited staining (fig. 3C). Upon dissection of siliques, GUS staining could be seen in the vasculature of the valves and septum and in the funiculus (fig. 3, E and F). The *YSL3* reporter was observed in floral tissues only in anthers and pollen grains (fig. 3, J and K). Confirmation of reporter gene activity in floral tissues was accomplished by RT-PCR analysis (fig. 3M). *YSL1* transcript was detected in flowers, floral buds, and less abundantly in siliques, whereas the *YSL3* message was detected in flowers and floral buds only. These expression patterns support roles for YSL1 and YSL3 in supplying metal-NA to reproductive tissues.

Double Mutants Have Low Fertility

As the *ysl1ysl3* double mutants reached the reproductive stage, another aspect of the mutant phenotype became apparent. We observed that most of the flowers on the mutant plants did not develop siliques, and of those siliques that did develop, there were few seeds inside. To test whether defective pollen was at least partially responsible for the fertility defect, we removed anthers from Col-0 and *ysl1ysl3* flowers and stained them for pollen

viability. The results clearly indicated that most of the pollen grains within the anthers of *ysl1ysl3* fail to develop into viable pollen (fig. 4, A and B). However, upon seed harvest, we noticed that many of the ovules that were fertilized and developed into seeds produced abnormally shaped and small-sized seeds, with Col-0 seeds weighing an average of 29 µg and *ysl1ysl3* seeds weighing an average of 16 µg. Viability of the *ysl1ysl3* seeds was quite low in comparison to Col-0. In germination tests on MS agar, *ysl1ysl3* seeds germinated at 18%, as compared to a seed germination rate of 93% for Col-0. Some of the seeds were imbibed and dissected to observe the embryo that they contained. We noticed that, in many cases, embryo development was arrested prematurely (fig. 4C), which may explain *ysl1ysl3* low seed viability.

Double Mutants Have Low Metal Content

Because *ysl1ysl3* plants exhibited chlorosis symptoms typical of metal deficiency, we measured mineral concentrations in the plants. Wild-type Col-0, *ysl1*, *ysl3*, and *ysl1ysl3* plants were used for elemental analysis of shoots of plants grown on MS agar. Plants were grown for 18 d, whereupon the *ysl1ysl3* plants exhibited interveinal chlorosis, whereas both single mutants and the wild type remained green. Plants were harvested and metal concentrations plotted relative to Col-0 (fig. 5, A and B). Metal concentrations did not differ between *ysl1*, *ysl3*, and Col-0. Mn, cobalt (Co), and Cu concentrations of plate-grown plants were similar to wild-type levels in *ysl1ysl3*. However, Fe concentration was decreased by 23% in *ysl1ysl3* shoots and was 36% lower the roots. This indicates that, under these conditions, the cause of chlorosis in the *ysl1ysl3* plate-grown plants was Fe deficiency. Interestingly, molybdenum (Mo) concentration was increased in *ysl1ysl3* in both roots (42%) and shoots (48%).

   To follow up this experiment, we grew Col-0 and *ysl1yls3* plants in a commercial potting mix for 20 d and measured metal concentrations (fig. 5C). Although the *ysl1ysl3* plants were showing interveinal chlorosis, the mineral analysis results were different from those of plants grown on MS agar. In this case, Fe concentration was decreased by only 9%, which was not statistically different from wild type. However, Mn was increased by 47%, Zn by 28%, and Cu by 182%. Mo and Co concentrations were similar in both genotypes and were not considered in further experiments, with Co at 0.23 ± 0.06 in Col-0 and 0.30 ± 0.07 in *ysl1ysl3*, and Mo at 1.0 ± 0.5 in Col-0 and 1.0 ± 0.4 in *ysl1yls3*.

Double Mutants Have Regulated Fe Deficiency Signaling

Because *ysl1ysl3* plants have a leaf chlorosis phenotype resembling Fe deficiency (fig. 1) and Fe concentration is lower in agar-grown *ysl1ysl3* shoots

(fig. 5), we expected root Fe deficiency responses, such as *IRT1* Fe transporter expression and ferric reductase activity, to be increased. These parameters, and total chlorophyll concentration, were quantified in plants grown on MS media for 18 d. Despite the advanced chlorosis of *ysl1ysl3* plants, root ferric reductase activity of *ysl1ysl3* and Col-0 roots was nearly equal in both genotypes and the *IRT1* transcript was undetectable in both genotypes (data not shown). We suggest that this indicates an abnormality in these plant responses to low tissue Fe levels. If the plants were responding normally to reduced tissue levels of Fe, they should have up-regulated ferric reductase activity and IRT1 expression.

We further wondered whether the *ysl1ysl3* mutant was capable of up-regulating its Fe deficiency responses. This was tested by growing Col-0 and *ysl1ysl3* on MS plates for 14 d and then switching the plants to MS – Fe for 5 additional days, and measuring total chlorophyll and ferric reductase activity each day. Chlorophyll levels of *ysl1ysl3* were approximately one-half of Col-0 at the beginning of the experiment (fig. 6A) and dropped in both genotypes over the time course, reaching approximately equal levels on day 4. The *ysl1ysl3* plants did have an increase in root ferric reductase activity (fig. 6B), indicating that the roots can respond to Fe availability. The temporal pattern of reductase activity was similar to that of the Col-0 plants, although the activity reached was quite diminished in *ysl1ysl3*. Transcript levels of the Fe-regulated *IRT1* transporter were sampled after 3 and 4 d from transfer to MS + Fe or MS – Fe plates, with similar results in both genotypes (day 4 shown in fig. 6C), again indicating that *ysl1ysl3* can respond to Fe deficiency.

YSL1 *and* YSL3 *Roles in Leaf Senescence*

Data from microarray experiments in the AtGen- Express: Expression Atlas of Arabidopsis Development experiment by The Arabidopsis Functional Genomics Network (Schmid et al., 2005; http://www. uni-tuebingen.de/plantphys/AFGN) indicated that *AtYSL1* and *AtYSL3* are expressed at high levels during leaf senescence. To confirm this, we observed expression levels in senescing leaves. In one experiment, we artificially induced leaf senescence by detaching leaves and incubating them on deionized water in petri dishes in either light or darkness. Figure 7A shows that both *YSL1* and *YSL3* mRNA levels increased substantially as the leaves senesced. In addition, we compared YSL1-GUS and YSL3-GUS reporter expression in leaves at two time points. At 20 d after sowing, rosette leaf number 6 (the sixth true leaf to emerge) was stained for histochemical detection of GUS activity for 6 to 9 h (fig. 7, B and D). By monitoring chlorophyll concentration, we determined that day 38 was midway through leaf senescence (approximately 50% chlorophyll loss; data not shown). Leaf number 6 samples of *YSL1-GUS* and *YSL3-GUS* reporter lines were taken again on day 38 and

stained for 6 to 9 h (fig. 7, C and E). GUS activity was clearly elevated as compared to day 20, and the expression pattern had relocalized from the midvein only, at day 20, to the midvein, primary, and secondary veins and the cells surrounding these veins.

It is known that, during leaf senescence, nutrients, including most minerals, are mobilized from senescing leaves to other tissues (Himelblau and Amasino, 2001). We hypothesized that if YSL1 and YSL3 are metal-NA transporters up-regulated during senescence, they may play a role in nutrient mobilization from leaves. To test this, we sampled the distal half of leaves 5 and 6 of Col-0 and *ysl1ysl3* plants at 28 and 38 d after sowing and compared the changes in mineral concentration between these time points, similarly to Himelblau and Amasino (2001).As shown in figure 7F, *ysl1ysl3* was less efficient at mobilization of a number of metals, especially Mn, Zn, and Cu. A highly remobilized element that is expected to be unaffected by the *ysl1* and *ysl3* mutations, phosphorus (P), is plotted for comparison.

Fertility and Mineral Homeostasis Is Partially Rescued by Fe(III)-EDDHA

In our preliminary studies with *ysl1ysl3*, we hypothesized that the main defect was in Fe homeostasis, based on the chlorotic phenotype of the leaves. Lending support to this idea was our discovery that subirrigation of the potting mix with Sprint 138 fertilizer [active ingredient Fe(III)-EDDHA] caused a greening of the leaves and greatly increased seed set of the mutants. We conducted further experiments using subirrigation of Fe(III)-EDDHA and foliar application of Fe. Foliar Fe was applied to Col-0 and the mutants *ysl1ysl3* and *irt1* as ferric ammonium citrate. Ammonium citrate was applied as a control. The *irt1* mutant is defective in Fe uptake from the soil and can be rescued by soil amendment (Vert et al., 2002). Application of foliar Fe increased the chlorophyll concentration of both *irt1* and *ysl1ysl3* mutants, whereas little effect was seen for Col-0 (fig. 8A). Seed number was improved from < 1% to 44% of that of Col-0 for *irt1*, but only to 13% for Fe-treated *ysl1ysl3* plants (fig. 8B). A much greater increase in seed set was observed for *ysl1ysl3* plants treated by subirrigation of pots with Fe(III)-EDDHA (fig. 8C). In this case, seed set was improved to 57% of that of Col-0 plants. The Fe(III)-EDDHA treatment also greatly increased pollen production in *ysl1ysl3* plants (data not shown), which likely accounts for some or all of this increased fertility. Furthermore, the seeds from treated *ysl1ysl3* plants had much higher germination rates, both on soil (89% germination) and MS agar plates (92% germination), than the seeds from untreated plants (33% on soil; 74% on MS agar plates.)

Because chlorophyll levels and fertility were greatly restored by Fe(III)-EDDHA treatment, we also determined the effect of this fertilization on leaf

and seed metal concentrations. As seen previously (fig. 5C), *ysl1ysl3* mutant leaves had increased levels of Mn, Zn, and especially Cu (fig. 9A). Treatment with Fe(III)-EDDHA decreased leaf Mn and Zn concentrations in both *ysl1ysl3* and Col-0, whereas leaf Fe levels increased. Upon Fe(III)-EDDHA treatment, *ysl1ysl3* and Col-0 leaves had similar Mn, Fe, and Zn concentrations. Fe(III)-EDDHA treatment had no effect on the Cu levels of Col-0 shoots, but resulted in even greater Cu concentrations in *ysl1ysl3* leaves. Metal concentrations in the seeds showed markedly different patterns (fig. 9B). The seed concentration of Fe, Zn, and especially Cu was lower in the mutants than in Col-0 plants. Subirrigation of plants with Fe(III)-EDDHA led to a decrease in seed Zn concentration and an increase in seed Fe and Cu concentration. Notably, the Fe(III)- EDDHA treatment caused the level of seed Fe to rise to the same levels as contained in Col-0 plants, but seed Zn and Cu remained low in spite of the treatment. The level of seed Mn was decreased in both genotypes by Fe(III)-EDDHA treatment.

Discussion

YSLs as Metal-NA Transporters

The *AtYSL* gene family was identified in *Arabidopsis* following cloning and characterization of maize *YS1*. YS1 is a plasma membrane-localized transporter protein that is necessary for acquisition of Fe by uptake of Fe(III)-phytosiderophores (Curie et al., 2001) using a proton motive force-dependent mechanism (Schaaf et al., 2004). Although *Arabidopsis* cannot take up or synthesize phytosiderophores, it contains the structurally related nonprotein amino acid NA. NA has been implicated in metal homeostasis in a number of studies using the NA synthesis mutant *chln* of tomato (Stephan and Grun, 1989; Becker et al., 1992; Ling et al., 1999). Previous work in our lab has demonstrated that the maize YS1 protein transports Fe(II)-NA (Curie et al., 2001; Roberts et al., 2004). Furthermore, we have characterized *At*YSL2 as an Fe(II)-NA and Cu-NA transporter on the basis of complementation of the yeast (*Saccharomyces cerevisiae*) mutants *fet3fet4* and *ctr1* (Di-Donato et al., 2004), which are unable to grow on Fe- and Cu-limiting media, respectively. Expression of rice YSL2 in Xenopus oocytes provided evidence for transport of Fe(II)-NA and Mn(II)-NA (Koike et al., 2004). AtYSL1, AtYSL4, AtYSL5, AtYSL6, AtYSL7, and AtYSL8 also complement the Fe uptake defect of the yeast *fet3fet4* mutant when Fe(II)-NA is provided as a substrate (L.A. Roberts and E.L. Walker, unpublished data). Thus, we and others (Koike et al., 2004; Le Jean et al., 2005) hypothesize that the most likely role of YSL proteins are in transport of metal-NA complexes.

Functions of YSL1 *and* YSL3 *Revealed by the Double-Mutant Phenotype*

Several aspects of the *ysl1ysl3* double-mutant phenotype suggest Fe deficiency as the underlying defect. Yellowing between the veins is a classic symptom of Fe deficiency and this phenotype is corrected by the addition of Fe, either by subirrigation with Fe(III)- EDDHA or by foliar application of ferric ammonium citrate. Moreover, the overall level of Fe in both leaves and roots of plants grown on MS agar plates is slightly, but significantly, lower than normal. Le Jean et al. (2005) found that *ysl1* single mutants exhibit significant defects only in seeds, which had low Fe and NA content. The *ysl1* mutant seeds also exhibited a germination defect on low Fe medium. The levels of metals in leaves of *ysl1* single-mutant plants were normal, and NA levels in leaves were elevated only when the plants were grown on low-Fe medium. Likewise, the metal levels in *ysl3* plants are not significantly different from wild-type plants (fig. 5A). The finding that *ysl1ysl3* double mutants contain lower than normal levels of Fe in both leaves and seeds demonstrates that both YSL1 and YSL3 are necessary to maintain proper Fe homeostasis during vegetative and reproductive growth.

Other aspects of the *ysl1ysl3* double-mutant phenotype are inconsistent with the hypothesis that Fe deficiency is the sole underlying cause of the pleiotropic defects observed. Most notably, high levels of Cu in the leaves of *ysl1ysl3* double-mutant plants indicate an alteration in Cu homeostasis during vegetative growth of the double-mutant plants. Application of Fe does not completely alleviate the fertility defects exhibited by the double mutant. Furthermore, during leaf senescence, mobilization of Fe from the leaves is not markedly impaired, whereas mobilization of Zn and Cu is much lower than in wild-type plants. Consistent with this finding, the levels of Zn and Cu in the seeds of double-mutant plants are low in spite of elevated levels of these elements in leaves of the same plants. Thus, YSL1 and YSL3 have additional roles during leaf senescence and seed loading: They are required for efficient mobilization of Zn and Cu from leaves and into seeds.

Regulation of YSL1 *and* YSL3 *Gene Expression*

Regulation of the *YSL1* and *YSL3* genes (fig. 3) is similar to that of *YSL2* (Di-Donato et al., 2004). All three genes exhibit decreased expression in shoots during Fe-limited growth. We have hypothesized that this pattern reflects a role in sequestration or distribution of Fe from veins into mesophyll tissue in older leaves. Localization of YSLs has been observed in vascular parenchyma cells (fig. 3L; Koike et al., 2004; Le Jean et al., 2005), providing support for this model. During vegetative growth, decreased YSL expression during Fe deficiency may allow more Fe to remain in the vasculature, making it more

available to younger, actively growing tissues instead of being delivered to older tissues. We propose that a major physiological role of YSL1, 2, and 3 is to transport metal-NA complexes in vascular parenchyma cells. Further, we proposed that the specific role of YSL1 and YSL3 is to translocate metals through vascular parenchyma cells, especially in leaves, flowers, and fruits. Down-regulation of these genes in Fe-deficiency situations would decrease Fe removal from the xylem into adjacent tissues. This would facilitate exchange of Fe from xylem to phloem, which we hypothesize can occur without YSL1 and YSL3 activity. The increased phloem Fe would be delivered to the younger leaves, which are primarily supplied with nutrients from the phloem.

Consistent with data available from microarray experiments, we observed an increase in YSL1 and YSL3 expression in senescing leaves (fig. 7, A and B) and flowers. This timing of the highest expression levels, coupled with the decrease in metal mobilization during leaf senescence in the *ysl1ysl3* mutant, suggests that YSL family members are important for recycling of metals from senescing tissues. The *ysl1ysl3* double mutants mobilized a lower percentage of minerals overall, but this would be expected because the plants are chlorotic as compared to Col-0 and as such would have fewer sugars to drive phloem transport. This general mineral mobilization decrease can be detected in two of the minerals most highly mobilized from *Arabidopsis* leaves (Himelblau and Amasino, 2001); P was mobilized by 15% less in *ysl1ysl3* than wild type (fig. 7C), and potassium (K) 11% less (data not shown). However, the decrease in mobilization of several metals was significantly greater. Despite elevated Zn and Cu concentrations in leaves (figs. 5C and 9A), the *ysl1yls3* mutant was impaired in the mobilization of Zn by 43% and Cu by 82%. Surprisingly, Fe was mobilized proportionally similarly to P, indicating no significant defect in mobilization of Fe from leaves of *ysl1ysl3* plants. Possibly, Fe is mobilized at a different time point in the senescence program that our sampling was unable to detect. Alternatively, YSL1 and YSL3 may act directly in the veins of flowers and developing fruits and play no role in Fe mobilization from leaves.

We propose that the physiological role of YSL1 and YSL3 is to translocate metals into vascular parenchyma cells for distribution away from veins into interveinal regions in maturing leaves, away from interveinal regions toward phloem tissue in senescing leaves, and out of the vasculature in fruits to supply seeds. The YSLs could facilitate this flux across the tissues in either direction, depending on the metal concentration gradient at that stage of the life cycle. Presumably, YSL proteins are acting to take up metal-NA complexes into cells. Following uptake, the metals could move across the vascular parenchyma by symplastic routes, or unidentified metal efflux proteins may move metals or metal-NA complexes into the apoplastic space prior to uptake by neighboring cells. It is estimated that about 25% of the Fe in leaves is stored in the apoplastic space (for example, see Nikolic and

Romheld, 2003). This Fe might serve as part of the pool of Fe that is moved out of leaves during senescence. Obviously, the recycling of minerals from leaves during senescence is a complex process that requires coordination of many genes and proteins.

Effect of Fe-EDDHA Application

Fertility defects in *ysl1ysl3* double-mutant plants were reduced by application of Fe, either through the leaves as ferric ammonium citrate or through the soil as Fe(III)-EDDHA. Interestingly, soil application of Fe(III)-EDDHA was much more effective in restoring fertility than was application of Fe-citrate to the leaves (fig. 8). We presented evidence that foliar application of Fe is quite effective in restoring both chlorophyll content and fertility to the *irt1-1* mutant, which has a straightforward defect in uptake of Fe from the soil. Because fertility of the Fe-citrate-treated *ysl1ysl3* double mutants was poor, even when chlorosis was reversed, we suspected that EDDHA was affecting metal homeostasis in unexpected ways when it was added to the soil. The effects of Fe(III)-EDDHA treatment were not restricted to increasing Fe in the plants (fig. 9). In both *ysl1ysl3* and Col-0, Fe(III)-EDDHA treatment decreased Mn and Zn concentrations, while always increasing Fe and generally increasing Cu concentrations. Thus, in addition to raising the concentration of Fe in vegetative tissues, Fe-EDDHA treatment of the plants unintentionally lowered the concentration of Zn and Mn, two metals that are abnormally high in the double mutant. We speculate that decreased levels of Zn and Mn may be partly responsible for the restored fertility observed following Fe-EDDHA treatment, and that Fe-citrate fails to restore fertility to the same extent because the levels of Zn and Mn are not affected by this treatment.

We suggest two reasons why treatment with Fe- EDDHA might affect the levels of Zn and Mn in plants. The first is that the EDDHA interferes with uptake or translocation of Zn and Mn in some unknown way. To reveal this, it would be necessary to treat plants with EDDHA in the absence of Fe—an experiment that is currently not possible because Na-EDDHA has not been commercially available for several years. An alternative hypothesis is that Zn and Mn levels in the plant decrease when plants are provided with high levels of bioavailable Fe. This would occur due to down-regulation of the IRT1 Fe uptake transporter, which takes up not only Fe but also Zn and Mn. When plants are continually Fe replete, IRT1 expression is expected to be low and, consequently, uptake of Mn and Zn would be reduced. It has been well documented that plants experiencing Fe deficiency typically contain high levels of Zn and Mn (Lahner et al., 2003).

Comparison to NA-Less Plants

NA has been implicated as important for translocation of Cu, Fe, Mn, and Zn (Pich et al., 1994; Stephan et al., 1994; Pich and Scholz, 1996). The roles of NA in plants have been deduced in large part by study of the tomato mutant *chln*, which cannot synthesize NA (Ling et al., 1999). In a recent study, a NA-free tobacco mutant was generated by expressing the barley NAAT gene (Takahashi et al., 2003). The *ysl1ysl3* mutant has similarities to both *chln* and *NAAT* tobacco. In these mutants, an interveinal chlorosis phenotype is observed, fertility is impaired, and alteration of metal accumulation occurs. However, some important differences can be noted. The appearance of chlorosis in *naat*-tobacco and *chln* occurs in the youngest leaves, whereas in *ysl1ysl3* the young leaves are not noticeably more chlorotic than older leaves. This may be explained by the pattern of *YSL1* and *YSL3* expression, as indicated by GUS reporter activity, which is low in young leaves but high in older leaves of seedlings (fig. 3G; data not shown). Fe deficiency root responses are up-regulated in *chln* even at adequate Fe supply to roots, whereas plate-grown *ysl1ysl3* plants (and hydroponic *ysl1ysl3* plants; data not shown) show low levels of *IRT1* expression and root ferric reductase activity (fig. 6). These responses can be induced in the double mutants, although the maximal value of ferric reductase is lower in the double mutant. This decrease in maximal activity may be due to lower reductant availability resulting from lower photosynthetic capacity in the chlorotic mutants. The *naat*-tobacco mutant leaves had low levels of Mn, Zn, and Cu, whereas soil-grown *ysl1ysl3* mutants had elevated Mn, Zn, and, especially, Cu levels (figs. 5C and 9A). These results further suggest that YSL1 and YSL3 may transport Mn-, Zn-, and Cu-NA.

Conclusion

The findings presented here have a number of important implications. The first is that losing the ability to transport Fe-NA complexes in vegetative tissues results in Fe deficiency. This highlights the essential role of Fe-NA transport in Fe homeostasis in plants. Failure of pollen and embryo development in the double mutant suggests that Fe acquisition via Fe- NA complexes is essential in reproduction. Finally, the finding that these YSL transporters are involved in mobilization of metals from leaves, and the suggestion that these mobilized metals are transported to and used by developing seeds, is an important clue to the molecular processes involved in metal accumulation in seeds.

Materials and Methods

Plant Growth Conditions

Seeds were surface sterilized with bleach and imbibed at 4°C for 4 to 5 d. Square petri plates containing 25 mL of 1% agar made with MS media and 1% Suc were used for sterile culture. Plates were positioned in an upright position so that the roots grew along the surface rather than inside the agar, which allowed for easy transfer or removal of agar-free roots for elemental analysis. For metal deficiency treatments, desired metals were left out of the agar mixture, as indicated. Soil-grown plants were sown directly onto commercial potting mix (Promix) or transferred from petri plates after 7 to 10 d of growth. Growth chamber conditions for plates and soil-grown plants were 16-h photoperiod at 22°C.

For Sequestrene supplementation experiments, Col-0 and *ysl1ysl3* plants were divided into two groups, one-half of which were subirrigated with tap water and one-half of which were subirrigated with 0.5 mg/L Sequestrene (Sprint 138; Becker-Underwood). Plants were allowed to grow to maturity and seeds were harvested. Weight per seed was determined based on a sampling of weights of 100 seed batches. Percentage viability of seeds was determined 7 d after sowing. A seed was deemed viable if both cotyledons and root were present. Pollen viability was determined as described (Alexander, 1969).

Foliar application of Fe was performed by spraying a 2 mg/mL solution of Fe ammonium citrate (Sigma) directly onto the aboveground portions of the plants. Control plants were sprayed with a 2 mg/mL solution of ammonium citrate. Spraying commenced when the first true leaves emerged from seedlings and continued every 3 to 4 d throughout the rest of the plant's life cycle.

Germination tests were performed by surface sterilizing seeds and allowing them to imbibe at 4°C for 48 to 72 h. One hundred seeds were then either plated onto standard MS agar or in planted commercial potting mix (Promix). Seeds were allowed to germinate for 1 week, at which time germination was scored as successful emergence of the hypocotyls and cotyledons.

DNA Manipulations

PCR primers used are listed in table 1. *YSL1* and *YSL4*, *6*, and *8* cDNAs were amplified by RT-PCR and cloned into pDESTY, a Gateway-modified version of pFL61. Total RNA was prepared from leaves of mature, flowering plants using the Qiagen RNeasy plant kit. Two micrograms of RNA was reverse transcribed using SuperScriptII (Invitrogen), and one-tenth of the resulting cDNA was used as a template in a PCR reaction using Expand High- Fidelity polymerase (Roche). Primers were modified to contain attB recombination sites (Gateway System; Invitrogen) or TOPO (Invitrogen) cloning sites. The amplified products were introduced into plasmids pDONR201 or pENTRdTOPO (Invitrogen), and the resulting clones verified by complete sequencing. The yeast (*Saccharomyces cerevisiae*) expression vector pFL61 (Minet et al., 1992) was modified to contain the Gateway recombination cassette, RFC-B (Invitrogen) to create pDESTY. cDNAs were cloned into pDESTY via LR recombination as described by the manufacturer (Invitrogen). The *YSL5* cDNA was obtained from the

Ecker size-selected 3-d hypocotyl library (obtained from the Arabidopsis Biological Resource Center [ABRC]) and cloned in pFL61. A full-length cDNA for *YSL7* was obtained as expressed sequence tag M67I025TM.

Mineral Analysis

Plant tissue was placed in Pyrex digestion tubes and the digestion was carried out using 1 mL HNO_3 at 114°C for 4 h. The Pyrex tubes were pretreated with HNO_3 under normal digestion conditions to decrease the background signals. Each case was then diluted to 10 mL and analyzed on a Perkin-Elmer Elan DRC-e inductively coupled plasma mass spectrometer using a glass Conikal nebulizer drawing 1 mL/min. The collision cell gas was methane and was used only for Fe.

For plate-grown plants, Col-0, *ysl1*, *ysl3*, and *ysl1ysl3* seeds were sown onto MS agar plates as described above. After 18 d, roots and shoots were separated, dried in a 60°C oven, and weighed. Mineral analysis was performed as described above.

RT-PCR

Total RNA was isolated using the RNeasy kit (Qiagen) from fresh tissues or tissues flash frozen in liquid N_2 and stored at –80°C. RNA was DNase treated (Ambion) and quantified by UV spectroscopy. One microgram of total RNA was reverse transcribed using SuperScriptII (Invitrogen), and the RT reaction was used directly as a template for a 50-μL PCR reaction. Primers used are indicated in table 1. The *YSL1* primer set was used with a 100-ng template (based on the starting amount of RNA), and PCR was carried out for 30 cycles for shoots and floral parts and 35 cycles for roots. The amount of template for *YSL3* was 50 ng and PCR was for 30 cycles. *YSL1* and *YSL3* forward primers were designed to span an intron; thus, they were inefficient in amplifying genomic DNA and would produce a different size product if genomic amplification did occur. Amplification of genomic DNA was not observed in any of the reactions. The *IRT1* primer set was used with a 100-ng template for 30 cycles. Control primers for *18S* rRNA were used on a 5-ng template for 30 cycles. As an additional control for genomic DNA contamination, 100 ng of RT reactions minus RT enzyme was used in PCR reactions with an *18S* primer set and failed to produce bands after 30 cycles. PCR conditions were as follows: an initial denaturation step of 95°C for 3 h, followed by cycles of 95°C for 30 min, 64°C for 30 min (60°C for *IRT1*), 72°C for 1 h, with a final elongation cycle of 7 h. The correct cycle number was determined by observing results of PCR on ethidium bromide-stained gels.

Ferric Reductase Assay and Chlorophyll Concentration

Col-0 and *ysl1ysl3* plants were grown on MS media for 18 d and then used for ferric reductase activity determination and chlorophyll concentration quantification. For Fe-deficiency treatments, plants were transferred to MS-Fe media on day 14, and 4 d later ferric reductase activity was determined. Ferric reductase activity of individual roots was determined by placing them in 1mL of buffer containing 0.2 mM $CaSO_4$, 5 mM MES, pH 5.5, and 0.2 mM Ferrozine (Sigma). The reaction was initiated by addition of Fe(III)-EDTA to a final concentration of 0.1 mM and allowed to

continue for 30 to 60 min, after which an aliquot was removed and A_{562} was determined. Roots were weighed and, if to be used for RT-PCR, were immediately flash frozen in liquid N_2. Shoots were excised and fresh weight was determined. Shoots were placed in 1 mL of *N,N'*-dimethylformamide and chlorophyll was extracted overnight. Total chlorophyll was determined as described by Inskeep and Bloom (1985).

GUS Reporter Gene Assays

The YSL1 promoter-GUS reporter gene was constructed as a translational fusion containing 1,663 bp upstream of the YSL1 start codon and the first 36 amino acids of the YSL1 protein. The YSL3 promoter-GUS reporter gene was constructed as a translational fusion containing 769 bp upstream of the YSL3 start codon and the first nine amino acids of the YSL3 protein. In both cases, the relevant fragment was amplified from genomic DNA using primers (table 1) that allowed recombination via the Gateway system (Invitrogen). The fragments were subsequently recombined into pDESTG2, a Gateway modified pPZP212 (Hajdukiewicz et al., 1994) vector containing GUS and nopaline synthase 3' downstream of the Gateway recombination cassette RFC-B (Invitrogen). Transgenic plants containing *YSL-GUS* reporter constructs were lightly prefixed in 10% acetone for 10 min to prevent diffusion of cellular content, then stained in GUS assay buffer [50 mM KPO_4, pH 7.0, 10 mM EDTA, 0.5 mM $K_3Fe(CN)_6$, 0.01% Triton X-100, 0.3 mg/mL (w/v) X-gluc (5-bromo-4-chloro-3-indolyl β-D-glucuronide); Rose Scientific] for 2 to 24 h. Staining was stopped by the addition of 70% (v/v) ethanol.

Table 1. Primers used in this study

| Primer Name	Sequence (5'–3')
Cloning primers	
YSL1 cDNA forward	CAGTCTCCATGGAAATAGAGCAAAGAAGG
YSL1 cDNA reverse	AAAACAGAGCATGAATCATCCGGATG
	AATATTTGAAGCTATACCAAGCATACAATCA
	ACTCCAAGCTTCGAGCGGCCGCCTTGGAAAA
YSL3 cDNA forward	AAATGAGGAGTATGATGATGGAGAGAGAGGG
	AAGCCGACAACCTTGATTGGAGACTTGACCA
	ATGGCGAAGAAGTCCAAAGCTTCGAGCGGCC
YSL3 cDNA reverse	GCTTAACTCGAATATTTACTCGGCATGAAGCC
YSL4 cDNA forward	TTGGAGTTATGGAGACGGAGATTCCTAGG
YSL4 cDNA reverse	TTCGTTGGTCAACCTTGTCTGTTTGAC
YSL6 cDNA forward	CTCAACATTTTCTCTTCCGCCATAACCAA
YSL6 cDNA reverse	TCCTTTTGTATGACTCACAGTTGCGGTTG
YSL8 cDNA forward	CTTGTTCACCATCTCTCTTATTTCGCAGAT
YSL8 cDNA reverse	CTTCTTCAACAGATCCATCTCATTGAGCTT
RT-PCR primers	
YSL1 RT forward	ACAAGGAGATGCACAGGCCAAGAAA
YSL1 RT reverse	TCACAGCCGCGATGACAAAAAGAC
YSL3 RT forward	ATTGGCCAGGAAACAAGTGTTTGGGT
YSL3 RT reverse	GACAAGTCCCGCGACTACACCATTT
IRT1 RT forward	GAGTCATTGCCATGGTCTTGGA
IRT1 RT reverse	GTATACTCAGCCTGGAGGATACAACCG
18s forward	CGGCTACCACATCCAAGGAA
18s reverse	GCTGGAATTACCGCGGCT
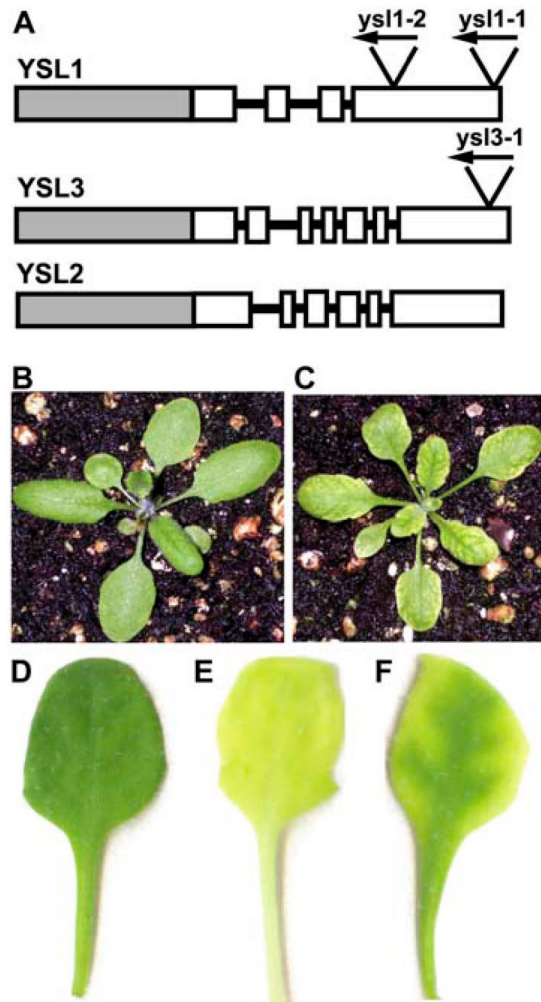
Figure 1. (A) Gene structure of *YSL1*, *YSL2*, and *YSL3*. Gray boxes represent promoter regions, white boxes represent exons, and lines represent introns (not to scale). Insertion sites of T-DNA and orientation are represented by triangles with arrowheads. The insertion in *ysl1-1* is within the *YSL1* gene but after the translational stop codon. (B) to (C), Three-week-old soil-grown plants. (B) Col-0 control plant. (C) Typical *ysl1ysl3* mutant. (D) to (F) Typical leaves of MS agar-grown plants 18 d after planting. (D) Col-0 control leaf. (E) Col-0 leaf from 18-d-old plant that was transferred to –Fe MS agar on day 14. (F) Typical leaf of *ysl1ysl3* grown on complete MS agar.
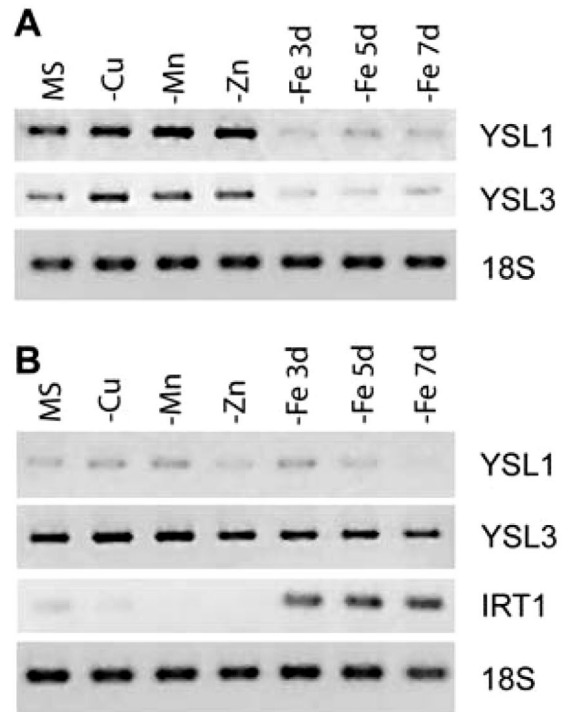
Figure 2. Expression of *YSL1* and *YSL3* is metal regulated. Col-0 plants were grown on complete MS for 7 d, then transferred to MS – Cu, Mn, or Zn for 7 d, or to MS – Fe for 3, 5, or 7 d. (A) RT-PCR using total RNA from shoots. Amplification of *YSL1*, *YSL3*, or 18S rRNA is shown. (B) RT-PCR using total RNA from roots. Amplification of *YSL1*, *YSL3*, or 18S rRNA is shown. As a positive control for Fe deficiency, *IRT1* was also amplified.
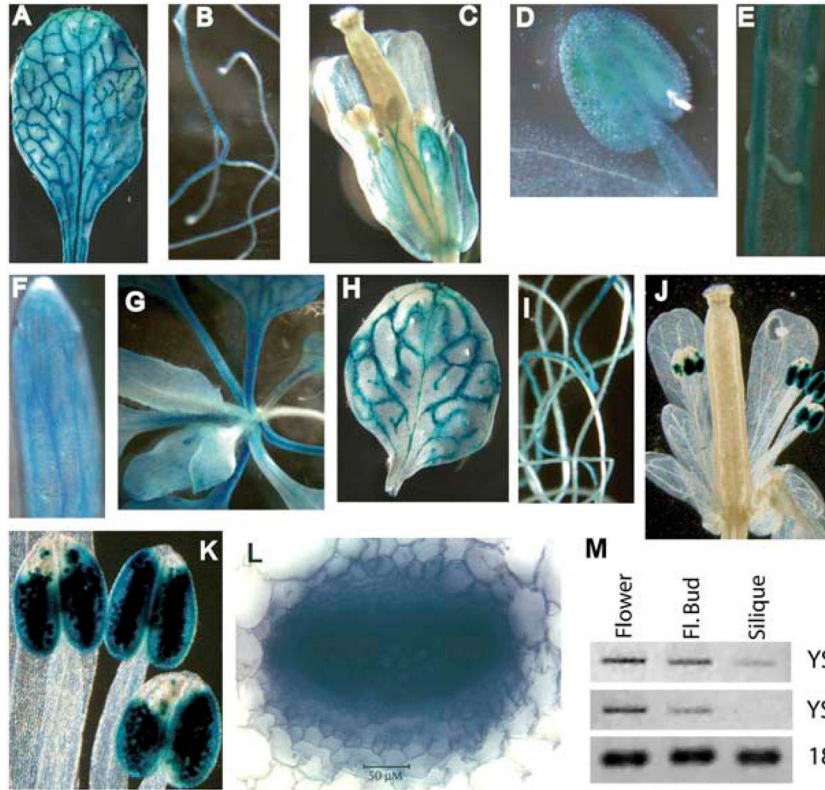
Figure 3. Localization of expression of *YSL1* and *YSL3* by GUS and RT-PCR. (A) to (G), Histochemical staining of *YSL1* promoter-GUS reporter plants. (A) Typical rosette leaf of soil-grown plant. (B) Roots of MS agar-grown plant. (C) Flower. (D) Immature stamen. (E) Septum and funiculi of opened silique with seeds removed. (F) Tip of valve of silique. (G) Rosette of soil-grown plant. Older leaves can be seen near the edges of photo; younger leaves are in center of photo. (H) to (L), Histochemical staining of *YSL3* promoter- GUS reporter plants. (H) Typical rosette leaf of soil-grown plant. (I) Roots of MS agar-grown plant. (J) Flower. (K) Stamens of mature flower. (L) Cross-section of petiole. (M) RT-PCR using total RNA from open flowers, floral buds, and siliques. Amplification of *YSL1*, *YSL3*, and 18S rRNA is shown.
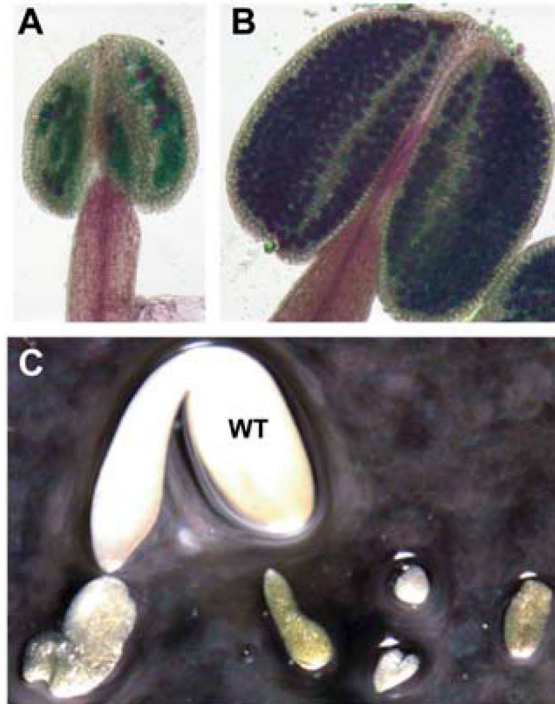
Figure 4. Pollen and embryo development is arrested in *ysl1yls3* mutants. (A) to (B), Anthers stained for pollen viability. Viable pollen grains are stained magenta. (A) Anther of *ysl1ysl3* double mutant plant. (B) Anther of Col-0 plant. (C) Embryo arrest in seeds of *ysl1ysl3*. Seeds were imbibed, then dissected. Embryo from Col-0 (marked WT) surrounded by examples of embryos from *ysl1ysl3* seeds.
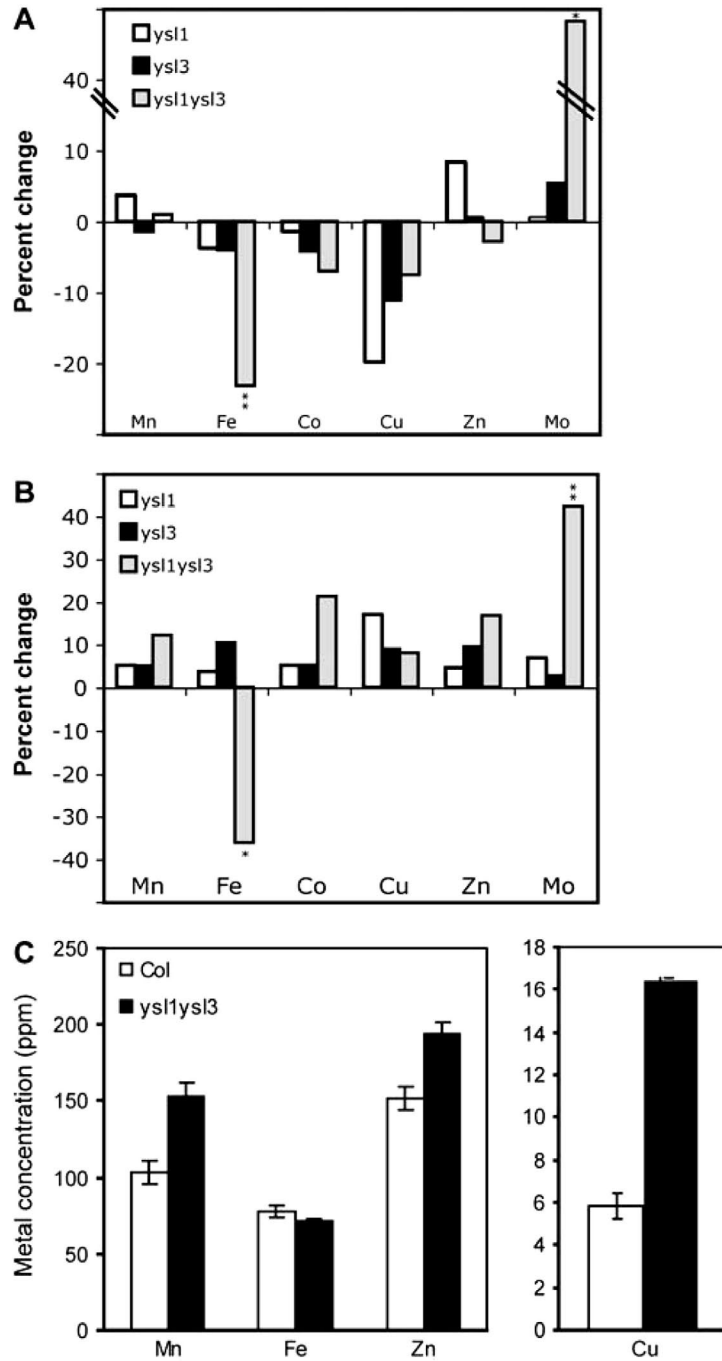
Figure 5. Metal concentrations of wild-type and *ysl1ysl3* plants. (A) and (B), Metal concentrations of plants grown on MS agar for 18 d. Results are given as percentage change in mutant (*n* ≥ 9) compared to wild type (*n* ≥ 9). *, Significance at *P* ≤ 0.05; **, significance at P ≤ 0.01. (A) Metal concentrations of shoots. Ranges of concentrations (in ppm) were Mn, 259 to 273; Fe, 54 to 70; Co, 0.65 to 0.70; Cu, 3.9 to 4.8; Zn, 151 to 168; and Mo, 3.6 to 5.3. (B) Metal concentrations of roots. Ranges of concentrations (in ppm) were Mn, 112 to 126; Fe, 713 to 1,234; Co, 1.6 to 1.9; Cu, 4.6 to 5.4; Zn, 1,104 to 1,289; and Mo, 3.1 to 4.4. (C) Metal concentrations of leaves of plants grown for 20 d on commercial potting mix. Results are given as ppm (*n* ≥ 9).
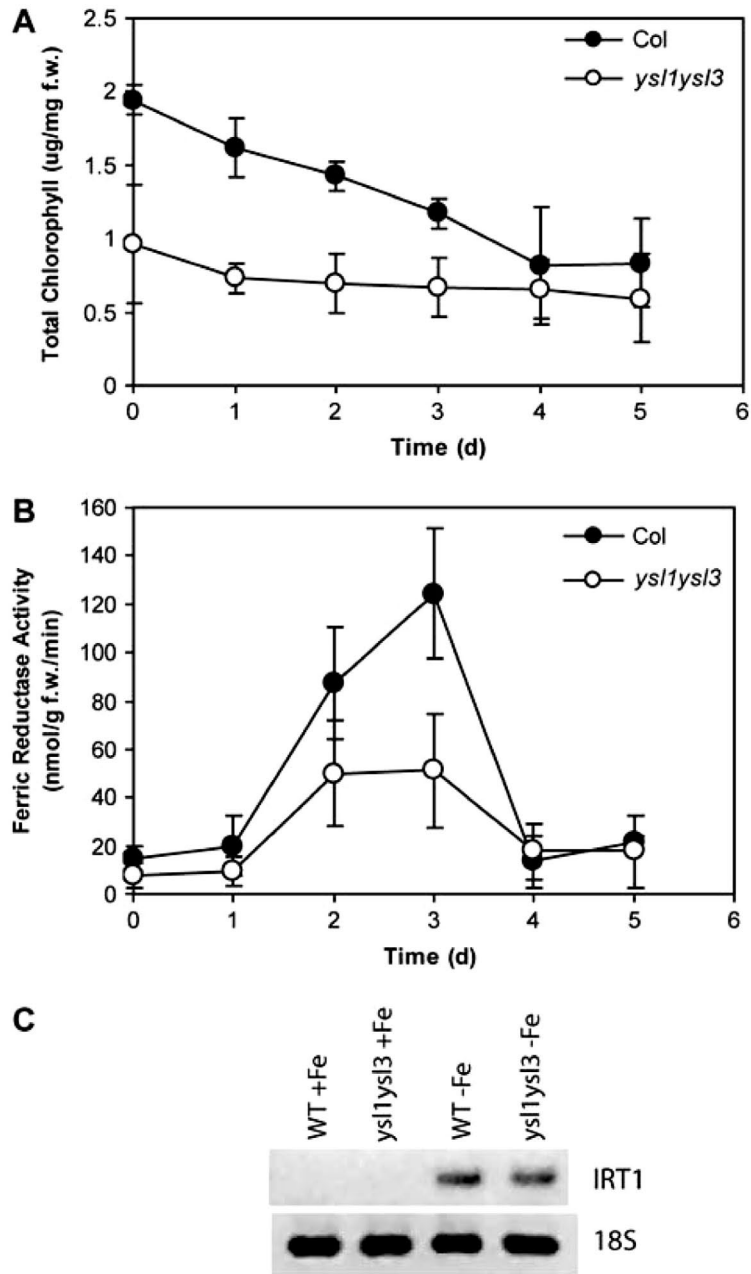
Figure 6. Fe deficiency responses in wild-type and *ysl1ysl3* plants. (A) Total chlorophyll concentration of shoot systems of plants grown on MS agar for 14 d, then transferred to MS-Fe agar for 0 to 5 d. (B) Root ferric reductase activity of plants grown on MS agar for 14 d, then transferred to MS-Fe agar for 0 to 5 d. (C) Semiquantitative RT-PCR of IRT1 mRNA levels in Col-0 and *ysl1ysl3* roots. Plants were grown on MS agar (+Fe) for 18 d or on MS agar (–Fe) for the final 4 d. Amplification of 18S rRNA is shown as a control for equal template loading.
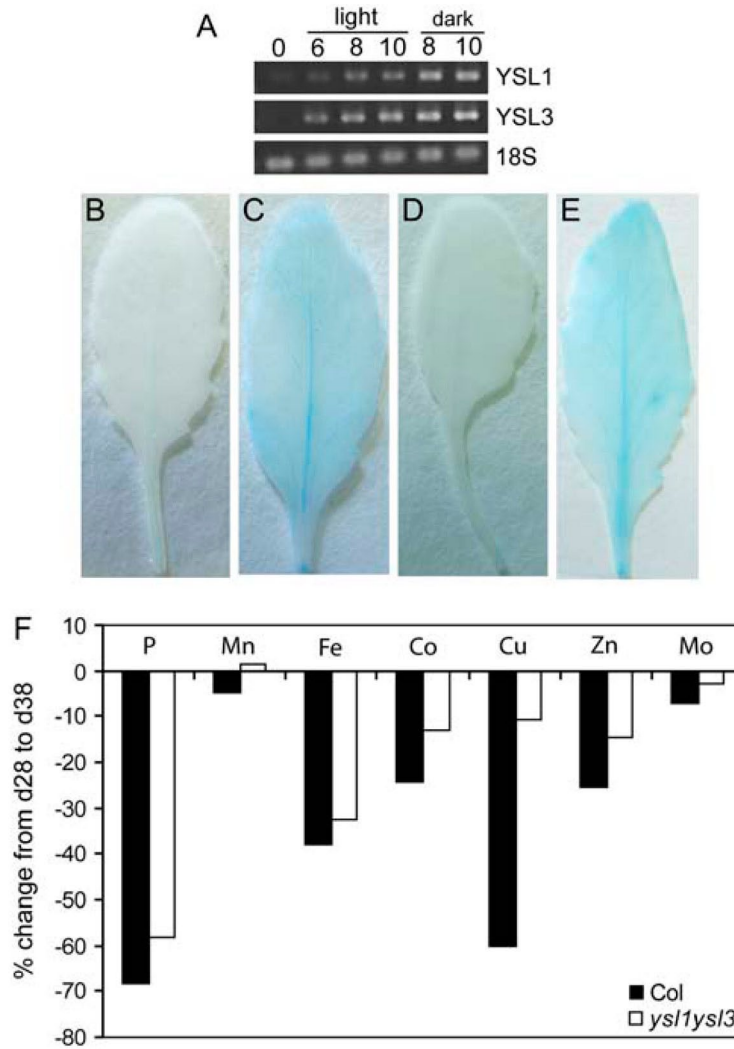
Figure 7. (A) Semiquantitative RT-PCR of *YSL1* and *YSL3* in senescing leaves. Detached leaves were incubated on deionized water in either light or darkness to induce senescence. (B) to (E), Histochemical staining of *YSL1* and *YSL3* promoter-GUS reporter plants during leaf senescence. Rosette leaf number 6 (the sixth true leaf to emerge) was stained for histochemical detection of GUS activity for 6 to 9 h. (B) Leaf of a *YSL1-GUS* plant at day 20. (C) Leaf of a *YSL1-GUS* plant at day 38. (D) Leaf of a *YSL3-GUS* plant at day 20. (E) Leaf of a *YSL3-GUS* plant at day 38. (F) Change in leaf metal concentration during senescence. The distal half of leaves 5 and 6 of Col-0 and *ysl1ysl3* plants was collected at 28 and 38 d after sowing and ions were measured by inductively coupled plasma mass spectrometry. Values are expressed as the percent difference in metal concentration from day 28 to day 38. The *t* test of the percent change arrays indicates no significant difference between the two genotypes for Mn, Fe, Co, or Mo, but $P < 0.05$ for Zn and $P < 0.01$ for P and Cu.
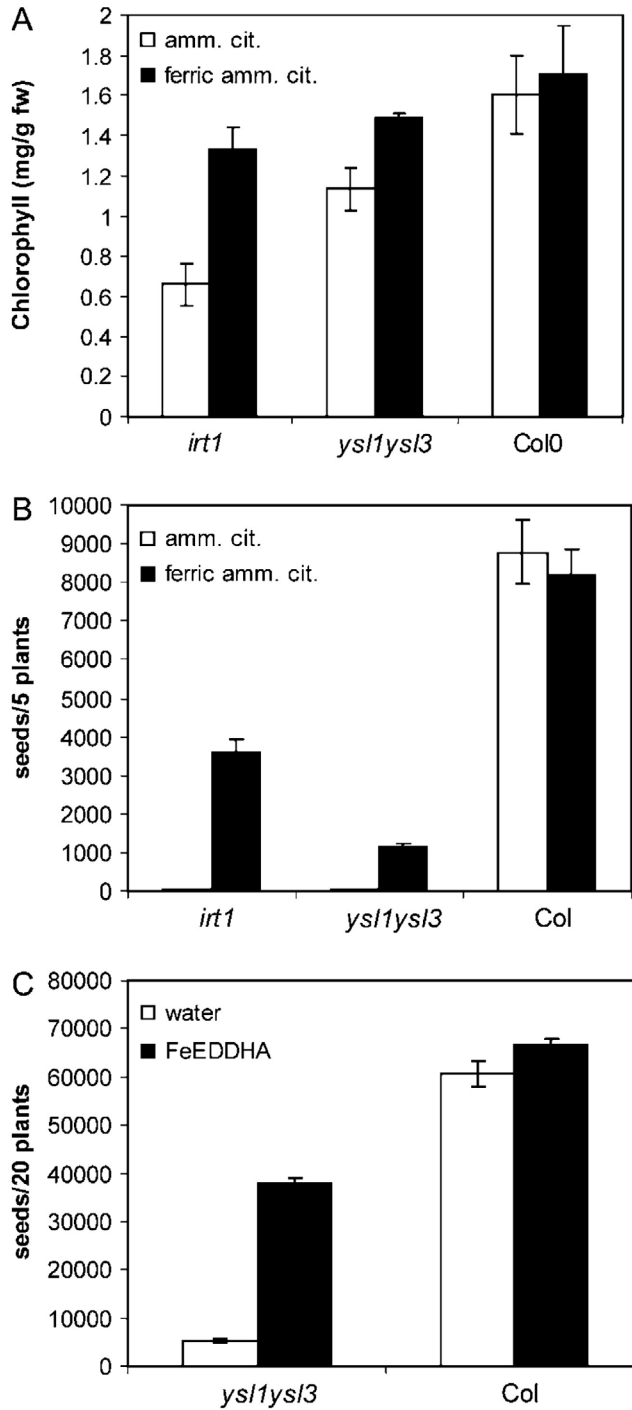
Figure 8. Responses of wild-type, *irt1-1*, and *ysl1ysl3* plants to alternative methods of Fe supplementation. (A) Total chlorophyll concentration of shoot systems of plants receiving foliar treatment of ferric ammonium citrate (black bars) or ammonium citrate (white bars). (B) Seed production by plants receiving foliar treatment of ferric ammonium citrate (black bars) or ammonium citrate (white bars). (C) Seed production by plants receiving subirrigation treatment with Fe-EDDHA (black bars) or plain water (white bars).
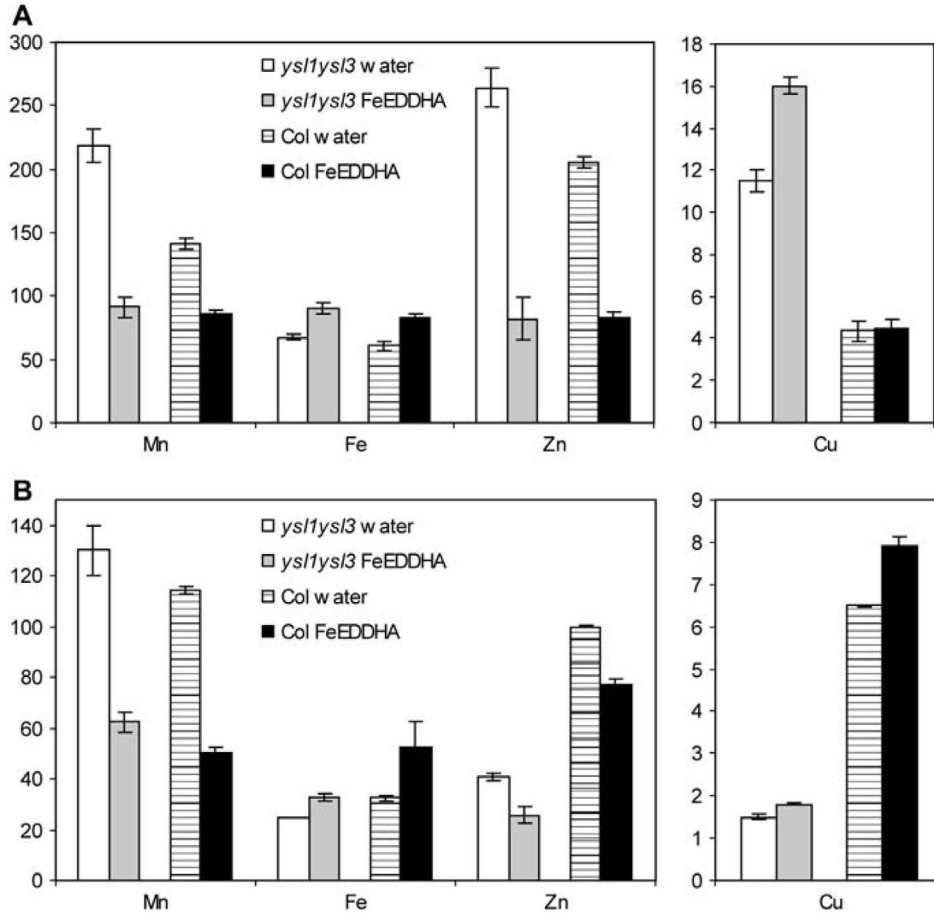
Figure 9. Metal concentrations of wild-type and *ysl1ysl3* plants following Fe-EDDHA treatment. (A) Metal concentrations of leaves. Results are given as ppm (*n* = 10). (B) Metal concentrations of seeds. Results are given as ppm (*n* = 4).

Literature Cited

Alexander MP (1969) Differential staining of aborted and non-aborted pollen. *Stain Technol* 44: 117–122.

Becker R, Grun M, Scholz G (1992) Nicotianamine and the distribution of iron into the apoplasm and symplasm of tomato (*Lycopersicon esculentum* Mill.). *Planta* 187: 48–52.

Bughio N, Yamaguchi H, Nishizawa N, Nakanishi H, Mori A (2002) Cloning an iron-regulated metal transporter from rice. *J Exp Bot* 53: 1677–1682.

Cary EE, Norvell WA, Grunes DL, Welch RM, Reid WS (1994) Iron and manganese accumulation by the *brz* pea mutant grown in soils. *Agron J* 86: 938–941.

Cohen CK, Garvin DF, Kochian LV (2004) Kinetic properties of a micronutrient transporter from *Pisum sativum* indicate a primary function in Fe uptake from the soil. *Planta* 218: 784–792.

Curie C, Briat JF (2003) Iron transport and signaling in plants. *Annu Rev Plant Biol* 54: 183–206.

Curie C, Panaviene Z, Loulergue C, Dellaporta SL, Briat JF, Walker EL (2001) Maize *yellow stripe1* encodes a membrane protein directly involved in Fe(III) uptake. *Nature* 409: 346–349.

Delhaize E (1996) A metal-accumulator mutant of *Arabidopsis thaliana*. *Plant Physiol* 111: 849–855.

DiDonato RJ Jr, Roberts LA, Sanderson T, Eisley RB, Walker EL (2004) Arabidopsis *Yellow Stripe-Like2* (*YSL2*): a metal-regulated gene encoding a plasma membrane transporter of nicotianamine-metal complexes. *Plant J* 39: 403–414.

Eckhardt U, Mas Marques A, Buckhout TJ (2001) Two iron-regulated cation transporters from tomato complement metal uptake-deficient yeast mutants. *Plant Mol Biol* 45: 437–448.

Eide D, Broderius M, Fett J, Guerinot ML (1996) A novel iron-regulated metal transporter from plants identified by functional expression in yeast. *Proc Natl Acad Sci USA* 93: 5624–5628.

Green LS, Rogers EE (2004) FRD3 controls iron localization in *Arabidopsis*. *Plant Physiol* 136: 2523–2531.

Grotz N, Fox T, Connolly E, Park W, Guerinot ML, Eide D (1998) Identification of a family of zinc transporter genes from *Arabidopsis* that respond to zinc deficiency. *Proc Natl Acad Sci USA* 95: 7220–7224.

Grusak MA, Pezeshgi S (1996) Shoot-to-root signal transmission regulates root Fe(III) reductase activity in the *dgl* mutant of pea. *Plant Physiol* 110: 329–334.

Grusak MA, Welch RM, Kochian LV (1990) Physiological characterization of a single-gene mutant of *Pisum sativum* exhibiting excess iron accumulation. *Plant Physiol* 93: 976–981.

Guerinot ML (2000) The ZIP family of metal transporters. *Biochim Biophys Acta* 1465: 190–198.

Hajdukiewicz P, Svab Z, Maliga P (1994) The small, versatile, *pZP* family of Agrobacterium binary vectors for plant transformation. *Plant Mol Biol* 25: 989–994.

Hell R, Stephan UW (2003) Iron uptake, trafficking and homeostasis in plants. *Planta* 216: 541–551.

Higuchi K, Suzuki K, Nakanishi H, Yamaguchi H, Nishizawa NK, Mori S (1999) Cloning of nicotianamine synthase genes, novel genes involved in the biosynthesis of phytosiderophores. *Plant Physiol* 119: 471–480.

Higuchi K, Watanabe S, Takahashi M, Kawasaki S, Nakanishi H, Nishizawa NK, Mori S (2001) Nicotianamine synthase gene expression differs in barley and rice under Fe-deficient conditions. *Plant J* 25: 159–167.

Himelblau E, Amasino RM (2001) Nutrients mobilized from leaves of *Arabidopsis thaliana* during leaf senescence. *J Plant Physiol* 158: 1317–1323.

Inoue H, Higuchi K, Takahashi M, Nakanishi H, Mori S, Nishizawa NK (2003) Three rice nicotianamine synthase genes, *OsNAS1*, *OsNAS2*, and *OsNAS3* are expressed in cells involved in long-distance transport of iron and differentially regulated by iron. *Plant J* 36: 366–381.

Inskeep WP, Bloom PR (1985) Extinction coefficients of chlorophyll *a* and *b* in *N*, *N*-dimethylformamide and 80% acetone. *Plant Physiol* 77: 483–485.

Kobayashi T, Nakanishi H, Takahashi M, Kawasaki S, Nishizawa NK, Mori S (2001) In vivo evidence that Ids3 from *Hordeum vulgare* encodes a dioxygenase that converts 2′-deoxymugineic acid to mugineic acid in transgenic rice. *Planta* 212: 864–871.

Koike S, Inoue H, Mizuno D, Takahashi M, Nakanishi H, Mori S, Nishizawa NK (2004) OsYSL2 is a rice metal-nicotianamine transporter that is regulated by iron and expressed in the phloem. *Plant J* 39: 415–424.

Lahner B, Gong J, Mahmoudian M, Smith EL, Abid KB, Rogers EE, Guerinot ML, Harper JF, Ward JM, McIntyre L, et al (2003) Genomic scale profiling of nutrient and trace elements in *Arabidopsis thaliana*. *Nat Biotechnol* 21: 1215–1221.

Le Jean M, Schikora A, Mari S, Briat JF, Curie C (2005) A loss-of-function mutation in AtYSL1 reveals its role in iron and nicotianamine seed loading. *Plant J* 44: 769–782.

Li L, Cheng X, Ling HQ (2004) Isolation and characterization of Fe(III)- chelate reductase gene *LeFRO1* in tomato. *Plant Mol Biol* 54: 125–136.

Ling HQ, Koch G, Baumlein H, Ganal MW (1999) Map-based cloning of chloronerva, a gene involved in iron uptake of higher plants encoding nicotianamine synthase. *Proc Natl Acad Sci USA* 96: 7098–7103.

Minet M, Dufour ME, Lacroute F (1992) Complementation of *Saccharomyces cerevisiae* auxotrophic mutants by *Arabidopsis thaliana* cDNAs. *Plant J* 2: 417–422.

Nikolic M, Romheld V (2003) Nitrate does not result in iron inactivation in the apoplast of sunflower leaves. *Plant Physiol* 132: 1303–1314.

Pich A, Scholz G (1996) Translocation of copper and other micronutrients in tomato plants (*Lycopersicon esculentum* Mill.): nicotianamine-stimulated copper transport in the xylem. *J Exp Bot* 47: 41–47.

Pich A, Scholz G, Stephan UW (1994) Iron-dependent changes of heavy metals, nicotianamine, and citrate in different plant organs and in the xylem exudate of two tomato genotypes. Nicotianamine as possible copper translocator. *Plant Soil* 165: 189–196.

Roberts LA, Pierson AJ, Panaviene Z, Walker EL (2004) *Yellow stripe1*. Expanded roles for the maize iron-phytosiderophore transporter. *Plant Physiol* 135: 112–120.

Robinson NJ, Procter CM, Connolly EL, Guerinot ML (1999) A ferricchelate reductase for iron uptake from soils. *Nature* 397: 694–697.

Rogers EE, Guerinot ML (2002) FRD3, a member of the multidrug and toxin efflux family, controls iron deficiency responses in *Arabidopsis*. *Plant Cell* 14: 1787–1799.

Schaaf G, Ludewig U, Erenoglu BE, Mori S, Kitahara T, von Wiren N (2004) ZmYS1 functions as a proton-coupled symporter for phytosiderophore- and nicoti-anamine-chelated metals. *J Biol Chem* 279: 9091–9096.

Schmid M, Davison TS, Henz SR, Pape UJ, Demar M, Vingron M, Scholkopf B, Wei-gel D, Lohmann JU (2005) A gene expression map of *Arabidopsis thaliana* devel-opment. *Nat Genet* 37: 501–506.

Schmidt W (2003) Iron solutions: acquisition strategies and signaling pathways in plants. *Trends Plant Sci* 8: 188–193.

Stephan UW, Grun M (1989) Physiological disorders of the nicotianamine auxotroph tomato mutant *chloronerva* at different levels of iron nutrition. II. Iron deficiency response and heavy metal metabolism. *Biochem Physiol Pflanz* 185: 189–200.

Stephan UW, Schmidke I, Pich A (1994) Phloem translocation of Fe, Cu, Mn, and Zn in *Ricinus* seedlings in relation to the concentrations of nicotianamine, an en-dogenous chelator of divalent metal-ions, in different seedling parts. *Plant Soil* 165: 181–188.

Stephan UW, Scholz G (1993) Nicotianamine: mediator of transport of iron and heavy metals in the phloem? *Physiol Plant* 88: 522–529.

Takahashi M, Terada Y, Nakai I, Nakanishi H, Yoshimura E, Mori S, Nishizawa M (2003) Role of nicotianamine in the intracellular delivery of metals and plant reproduc-tive development. *Plant Cell* 15: 1263–1280.

Vert G, Briat JF, Curie C (2001) *Arabidopsis* IRT2 gene encodes a root periphery iron transporter. *Plant J* 26: 181–189.

Vert G, Grotz N, Dedaldechamp F, Gaymard F, Guerinot ML, Briat JF, Curie C (2002) IRT1, an *Arabidopsis* transporter essential for iron uptake from the soil and for plant growth. *Plant Cell* 14: 1223–1233.

Waters BM, Blevins DG, Eide DJ (2002) Characterization of FRO1, a pea ferric-chelate reductase involved in root iron acquisition. *Plant Physiol* 129: 85–94.

Welch RM, LaRue TA (1990) Physiological characteristics of Fe accumulation in the "bronze" mutant of *Pisum sativum* L. cv "Sparkle" E107 (*brz brz*). *Plant Physiol* 93: 723–729.